Quo vadis, metasurfaces?

Journal:	*Nano Letters*
Manuscript ID	nl-2021-00828q.R3
Manuscript Type:	Mini Review
Date Submitted by the Author:	n/a
Complete List of Authors:	Qiu, Cheng-Wei; National University of Singapore, ECE Zhang, Tan; National University of Singapore, ECE Hu, Guangwei; National University of Singapore Faculty of Engineering, Electrical and Computer Engineering Kivshar, Yuri; Australian National University, Nonlinear Physics Center

Quo vadis, metasurfaces?

Cheng-Wei Qiu[1], Tan Zhang[1], Guangwei Hu[1], and Yuri Kivshar[2]

[1]Department of Electrical and Computer Engineering
National University of Singapore, Singapore 117583

[2]Nonlinear Physics Center, Research School of Physics
Australian National University, Canberra ACT 2601, Australia

Abstract:

The full manipulation of intrinsic properties of electromagnetic waves has become the central target in various modern optical technologies. *Optical metasurfaces* have been suggested for a complete control of light-matter interaction with subwavelength structures, and they have been explored widely in the last decade for creating next-generation multifunctional flat-optics devices. The current studies of metasurfaces have reached a mature stage where common materials, basic optical physics, and conventional engineering tools have been explored extensively for various applications such as light bending, metalenses, metaholograms, and many others. A natural question is where the future research on metasurfaces will be going: *Quo vadis, metasurfaces?* In this mini review, we provide perspectives on the future developments of optical metasurfaces. Specifically, we highlight recent progresses on hybrid metasurfaces employing low-dimensional materials, and discuss biomedical, computational and quantum applications of metasurfaces, followed by discussions of challenges and foreseeing the future of metasurface physics and engineering.

Corresponding authors:

Cheng-Wei Qiu, E-mail: chengwei.qiu@nus.edu.sg

Yuri Kivshar, E-mail: yuri.kivshar@anu.edu.au

Keywords: Metasurfaces, Two-dimensional materials, Biomedical optics, Optical computation, Quantum optics

Introduction

Metasurfaces are made of artificial subwavelength elements with small thickness, which provides powerful capability to manipulate waves[1–7]. Well before the exploration of metasurfaces, tailoring the light scattering with planar optical structures has majorly been pursued in diffractive optical elements, such as high-efficiency dielectric gratings[8] and space-variant Pancharatnam–Berry-phase-based diffraction gratings[9]. Nevertheless, the concept of metasurfaces provided much deeper insight and many more degrees of freedom to play with, for complete control of light. As one of the very first proposals, phase-discontinuity metasurfaces based on plasmonic V-shape nanoantennas with different geometries have been suggested and demonstrated to exhibit anomalous reflections and refractions governed by the generalized Snell's law [1], which stimulated a widespread interest of the optics community. Following this, new designs including those exploiting the geometric phases and dynamic phases have been proposed[10,11]; more materials such as dielectric materials and emerging materials have been explored[12]; tremendous new functionalities have been demonstrated including metalens[13], metaholograms[14–16], beam steering with nonlinear metasurfaces[17,18], versatile polarization generation[19], and many others. Nowadays, the study of metasurfaces grows rapidly reaching a new stage, blending various novel concepts, and exploring new materials for multiple cross-discipline applications.

General principles, functionalities, and applications of metasurfaces have been reviewed comprehensively in previous works[20–22]. Here, we aim to provide most recent perspectives on the future directions of metasurfaces and address emerging and promising fields of *optical metasurfaces* that are less emphasized previously. Therefore, in this mini-review, four major promising paths for the future development of metasurfaces are exclusively highlighted (see Fig. 1). Specifically, we provide an overview of metasurfaces integrated with low-dimensional materials, and then discuss metasurfaces for biomedical, computational and quantum applications. Firstly, hybridizing metasurfaces with two-dimensional (2D) materials, such as 2D Transition Metal DiChalcogenides (TMDCs)[23–28] and polar van der Waals (vdW) materials[29–31], can realize advanced manipulations of light-matter interactions at the nanoscale in a designer manner, offering a new platform for next-generation photonics. For new applications such as in biological systems, metasurfaces can largely enhance the sensitivity of biomolecular detection[32–35], distinguish chiral biomolecules[36], and achieve high-resolution bioimaging[37]. Another important trend is employing metasurfaces to process[38–48], optimize[49,50] and code information[51–54], which can perform mathematical computations and image processing. Finally, we discuss most recent applications of metasurfaces to quantum technologies. Meditated quantum entanglement[55–58] and a new platform for integrated quantum devices[59,60] may be possible with emerging metasurfaces. Nevertheless, these selected topics are exclusive, and we do not aim to cover all exciting trends in the study of metasurfaces. Other promising and paradigm-shift developments of metasurfaces, discussed in this perspectives, could be merging advanced computer algorithms[61,62] (machine learning, neural networks, and others), demonstrating topological physics and applications in flat metasurfaces[63], introducing time-variant metasurfaces to enrich dimensionality[64], combining metasurfaces with a micro-electro-mechanical system[65] (MEMS) and many other continuously emerging advances.

Hybridization with two-dimensional materials

One significant advance in developing new types of metasurfaces is to hybridize them with 2D and layered 2D materials. Beyond the general advantage of atomic thickness for ultracompact and ultrathin devices, those emerging nanomaterials offer exotic optoelectronic properties with rich physics and applications when interacting with photons. However, light-matter interaction in atomically thin materials is generally weak, so engineering their photonic behaviors and boosting their interactions with light are practical issues. Optical metasurfaces could allow the advanced manipulation of light-matter interaction in a designer manner, providing a nearly perfect engineering platform to fully unveil the great potentials of 2D materials in nanophotonics.

Figures 2a-b present examples of the hybridization of 2D TMDCs with metasurfaces. TMDCs are a representative kind of 2D materials with visible-frequency optoelectronic applications. Most 2D TMDCs present a direct bandgap in the visible and render the excitons when interacting with photons, with large excitonic binding energy. Besides, the broken time-reversal symmetry of the atomic structures induces the opposite Berry curvatures and pseudo-spins in the electronic band structures, lifting the valley degeneracy and resulting in a valley-contrast absorption and emission of spin-photons. Moreover, their broken inversion symmetry could allow the strong photonic spin-dependent second-harmonic generation (SHG), coupled to the interband transition in different valleys. Hybridizing the metasurface with 2D TMDCs can help to address the valley excitons and even their nonlinearity. Fig. 2a shows that a metasurface made of asymmetric plasmonic grooves would break the in-plane mirror symmetry, which supports the unidirectional propagation of surface plasmons excited by different circularly polarized in-plane dipoles[24]. This allows the excitons from different valleys with opposite pseudo-spins, strongly coupled to surface plasmons, to be separated and directed to opposite directions in the near field and at room temperature, promising the valleytronics and excitonic devices[24–26]. Differently, Fig. 2b illustrates a strategy of synthesizing metasurfaces with 2D TMDCs which exploits the coherent valley-contrast SHG process to address the valleys[27]. The plasmonic metasurface carries the geometric phase that is spin-dependent and boosts the light-matter interaction due to its strong field confinement[66]. The photons at the fundamental frequency, after being modified to carry the Pancharatnam-Berry phases by the metasurface, could access and pump the valleys coherently, resulting in SHG photons with a spin-valley-dependent geometric phase. Emission from the opposite valleys, boosted by the strong plasmonic localization, could be controllably separated, and steered to different directions, facilitating room-temperature valleytronics and nonlinear photonic devices.

Figures 2c-d show the hybridization of metasurface with layered 2D materials or polar vdW materials. Here, instead of simply synthesizing vdW materials with a metasurface, the hybridization strategy is implicit since it applies the advanced engineering in metasurface to the polar vdW materials for sophisticated photonic applications. Polar vdW nanomaterials can support the phonon polaritons (PhPs), which could be extremely anisotropic if the optical phonon frequencies at different crystal axis are separated enough, inducing the natural hyperbolicity[67]. Figure 2c shows that the grating metasurface of hexagonal boron nitride (hBN) can support the in-plane hyperbolicity, where the pristine hBN can only support in-plane isotropic PhPs[29]. In metasurface, the homogenization of structured materials can render exotic effective properties that are significantly different from their original ones. This concept is the root of hBN grating metasurface, where its in-plane isotropy can be broken to be extreme, allowing the hyperbolic PhPs propagation. Moreover, one can apply the rotation-induced engineering in twisted bilayer hyperbolic metasurface[68] to polar vdW materials. Fig. 2d shows that applying the metasurface's extreme dispersion engineering via the rotation[68], PhPs in twisted α-phase molybdenum trioxide (α-MoO_3) bi-layers can experience a hyperbolic-to-elliptic topological transition as the rotation angle changes, although each α-MoO_3 layer is in-plane hyperbolic[30,69–71]. Near the topological transition angle, the isofrequency contours necessarily become flattened, demonstrating a highly collimated polariton propagation, i.e., the polariton canalization. Such hybridization schemes are conceptual and allow to explore and utilize the metasurface concept to 2D materials and their layers.

Figures 2e-f depict light-matter interactions in the hybrid systems of excitonic 2D materials and plasmonic metasurfaces. Surface plasmons (SPs) excited in the metasurface can efficiently confine electromagnetic fields into deep-subwavelength volumes with highly enhanced field intensity, which, in turn, will strongly modify the light-matter interactions in excitonic 2D materials. Thus, excitons and SPs are coupled through coherent dipole-dipole interactions, and different coupling regimes are identified depending on the energy exchange rate between excitons and SPs. When the coupling becomes stronger and enters the intermediate regime, Fano-type interference is emergent and manifested as transparency resonances in the SP spectrum. As shown in Fig. 2e, the localized surface plasmon resonance of the bowtie metasurface is spectrally overlapped with the A-exciton resonance of MoS_2 monolayer at around 1.9 eV. As a result, a sharp and asymmetric feature resembling Fano lineshape is presented in the reflection spectra at around 1.9 eV, while the absorption of the MoS_2 monolayer is enhanced due to the strong plasmonic field[72]. Once the coherent coupling between SPs and excitons is dominant over all the loss channels, the strong coupling regime is achieved in the hybrid system. Then, two new mixed states possessing half-light-half-matter properties are formed and energetically separated by a Rabi splitting, which is manifested as a characteristic anticrossing of two branches. As depicted in Fig. 2f, a clear anticrossing of 18.2 meV is observed for the plasmonic cavity mode and the neutral exciton resonance of WSe_2 monolayer[73]. Such polaritonic devices promise great potential in ultrafast optoelectronics, all-optical logic, and low-threshold lasers.

Finally, the examples discussed above serve to showcase the general philosophy of hybridizing metasurface with 2D materials, which can be extended to many other emerging material platforms, including perovskites[74,75], phase changes materials[76], and even topological and quantum materials. For example, common challenges of conventional metasurfaces are losses and weak tunability, which however may be circumvented 2D materials. By incorporating a gain material, such as $MAPbI_3$ perovskite, with conventional metal-dielectric hyperbolic metasurface, its metal loss can be compensated so that the polarization anisotropy of emission can reach the same level as absorption[75]. Besides, the PhP responses are in principle immune to Ohmic losses offering a low-loss platform for nanophotonic metasurfaces. When combined with phase-change materials such as single-crystal vanadium dioxide (VO_2), the PhP metasurfaces with VO_2-hBN can facilitate the active and reconfigurable control of light in nanoscale[76]. Therefore, more exciting, and newer opportunities with hybridizing 2D materials and other emerging novel materials should be explored in the future.

Biomedical applications

Electromagnetic waves exhibit a rich yet safe range of interactions with biological systems from radio to optical wavelengths that are the basis for many biomedical technologies essential to modern life[77]. Therefore, besides incorporated low-dimensional materials, metasurfaces have also been harnessed to realize the next generation of biomedical devices that can rapidly and conveniently detect diagnostic signals and deliver medical treatments. They provide distinct capabilities being exploited to enhance the interface between engineered devices and biological systems. First, metasurfaces can concentrate electromagnetic fields at the deep subwavelength scale and resonantly amplify or suppress interaction with biological objects. Second, metasurfaces can freely tailor the electromagnetic response of a device, enabling wavefronts of the specific amplitude, phase, and polarization to be generated. Third, metasurfaces can be fabricated in flat and compact formats that can gain proximity to otherwise inaccessible physiological regions. The development of metasurfaces with such versatile capabilities has enabled advances in applications for biomedical sensing and imaging.

Optical techniques, such as infrared spectroscopy, are routinely used in biotechnology and medicine to analyze the molecular content of biological samples, in which changes in wavelength indicate the binding of specific biomolecules. The sensitivity of molecular detection is determined largely by the magnitude of optical change induced by a small concentration of the target molecule. The use of metasurfaces in biomolecular sensing can be traced to their ability to increase the strength of light-molecule interactions and convert biomolecular signals into changes in amplitude, wavelength, phase, and polarization of light for convenient readout. For example, metasurfaces composed of nanospheres, being capable of generating strong localized surface plasmon resonance, have emerged as an ideal platform for sensitive biomolecule detection[78] (Fig. 3a).

To further enhance the sensitivity, metasurfaces based on Fano resonance have been proposed thanks to the sharp intensity changes and extreme singularities of Fano lineshape. As shown in Fig. 3b, a biosensor based on Fano resonance has been demonstrated by asymmetry metasurface consisting of two plasmonic antennas in parallel and a perpendicular antenna coupler attached to one of them[32]. Two current modes were excited and coupled as electric dipole and quadrupole/magnetic dipole, corresponding to the super-radiant mode and subradiant mode, respectively. This asymmetric metasurface has shown the ability to determine the vibrational fingerprint and measurement of the thickness of the recognition protein. High sensitivity has also been achieved by a metasurface biosensor operating at a plasmonic exceptional point (Fig. 3c), where the sensitivity was enhanced by the nonlinear responses near the exceptional point[33]. In addition, hyperbolic metasurfaces have also been proposed for sensitive biomolecular sensing benefiting from the bulky modes and highly confined fields. Two typical architectures of hyperbolic metamaterials, parallel gold nanorod array[79] (Fig. 3d) and metal-dielectric multilayer[80] (Fig. 3e), have been demonstrated for biomolecular sensing using a streptavidin-biotin model.

Metasurfaces based on bound states in the continuum (BIC) have also been proposed for biomolecular detection[34,35], by which the high sensitivity has been achieved due to high-quality factors and strong field confinement of the metasurfaces. For example, a two-dimensional pixelated dielectric metasurface (Fig. 3f) has been proposed as an ideal platform for label-free and imaging-based molecule fingerprint detection[34]. The proposed dielectric metasurface (a-Si: H) consisted of a two-dimensional array of high-quality-factor pixels. Each pixel contains a zigzag resonator array recognized as supercavity modes driven by BIC, exhibiting a discrete resonant frequency linearly varied over a target mid-infrared fingerprint range. The pixel design of the metamaterial enabled molecular absorption signatures to be read out at multiple spectral points. The measured spectrum was then translated into a barcode-like spatial absorption map for imaging. Similar BIC-based metasurface combining with hyperspectral imaging has also been proposed to develop an ultrasensitive label-free analytical platform for biosensing[35]. Without using a spectrometer, this technique can acquire spatially resolved spectra from millions of image pixels and use smart data-processing tools to extract high-throughput digital sensing information.

Chiral metasurfaces can also be applied for chiral biomolecule sensing, which is important to distinguish different pharmacological potency and toxicity of chiral biomolecules with different handedness. Chiral metasurfaces can concentrate and tailor the near-field polarization of optical fields to generate super-chiral fields and amplify interactions with chiral molecules. As an example, a pair of plasmonic 'twisted' metasurface with opposite rotations (Fig. 3g) has been proposed to detect chiral biomolecules[36]. Two opposite responses corresponding to the opposite rotation of the metasurfaces were observed, which can be summed up to remove background signals and enhance the sensitivity of chiral biomolecular detection.

In addition to biosensing, metasurfaces can also play an important role in bioimaging. Benefiting from the subwavelength control, metasurface-based bioimaging systems can achieve high compactness as well as high imaging resolution. For example, a metasurface has been proposed as a metalens integrated into an optical coherence tomography (OCT) catheter[37] (Fig. 3h). The optical components at the distal end of the catheter were assembled using a custom-built platform comprised of holders for the metalens and traditional optical systems, such as fiber and prism. This metalens can tailor the phase such that it is free of spherical aberration and astigmatism, overcoming the essential barriers to diffraction-limit focusing and imaging. The building blocks of the metalens are amorphous silicon nanopillars, where each building block was distributed according to the calculated phase profile of a focusing spot with diffraction-limit resolution and free of chromatic dispersion, spherical aberration, and astigmatism. The imaging qualities of metalens endoscope and conventional OCT catheters were compared by imaging on fruit flesh and animal models (swine airways ex vivo and pulmonary airways of the sheep in vivo), both showing that the metalens endoscope captured images with higher qualities and more details.

Recently, a reconfigurable and intelligent metasurface imager has been proposed for high-accuracy microwave imaging and recognition of the human body[49] (Fig. 3i). Machine learning technology was applied and combined with the tunable metasurface to generate optimized radiation patterns in real time, which enabled high-speed data acquisition and high-quality imaging. The metasurface with operation frequency around 3 GHz was reprogrammable by tuning the meta-atoms, each of which was composed of three subwavelength-scale square metallic patches. Two adjacent patches were connected via a PIN diode that was digitally controlled by the applied bias voltage. The meta-atom supported four digitized phase levels by controlling the states of three diodes in a judicious combination. The metasurface was trained by the random projection and the principal component analysis. After being trained, the metasurface generated the optimized measurement mode in real-time to reconstruct a person, which was used to monitor the movement of the person. Recognition of human-body gestures was also demonstrated by the machine-learning metasurface imager with faster data acquisition compared to the random projection without training.

The above examples show the versatility of metasurfaces in biomedical sensing and imaging. The future development of metasurfaces for biomedicine could focus on solving the clinical problems by new designs and new mechanisms of metasurfaces, which could be the key components for future healthcare systems.

Computational and information metasurfaces

In addition to the interaction with biological systems, electromagnetic waves have also been widely used as an efficient and versatile information carrier for communication and signal processing[81]. With its compact structure, metasurface brings promising new possibilities in this direction. The computational and information metasurfaces are proposed to process information in systematic ways, thereby achieve functionalities like mathematical operation, computational imaging, wireless communication, etc.

The concept of computational metamaterial was proposed in 2014. It refers to metamaterials that can perform mathematical operations[38]. The concept was suggested for a metasurface sandwiched between two graded-index (GRIN) slabs (Fig. 4a). The GRIN slabs perform Fourier and inverse Fourier transformations, and the metasurface applies the required filtering in the momentum domain corresponding to the desired mathematical operator (Fig. 4b). The metasurface is a conceptual one and its realization may suffer from problems of low efficiency or complex structure. Therefore, considering these obstacles, a computational metasurface, which works high efficiently in reflection and consists of uncomplicated array structure, has been designed and experimentally demonstrated[39] to perform highly efficient spatial differentiation and integral based on gap-surface plasmons. The setup only requires one component to perform two Fourier transformations before and after the reflection.

However, the above metasurfaces still cannot perform analog computation by themselves because Fourier components are required to perform the operation in the momentum domain. A much simpler reflective design that directly works in the momentum domain makes use of the surface plasmon excitations in a Kretschmann configuration (a dielectric prism on a thin metal film)[40]. The system has a transfer function which approximates that of a first-order spatial differentiation at critical coupling, so it directly performs the operation without using any metastructure or Fourier components. Similarly, based on the intrinsic transfer function near a bound state in the continuum, a photonic crystal slab was theoretically proposed to perform a 2D Laplacian operation on normal incident fields in transmission[41]. Despite their simpler design, both schemes still require other components to facilitate the functioning of the 2D structure (a prism, in Ref.[40] and a dielectric slab, in Ref.[41]). Moreover, both schemes work in a small incident angle range and do not spare the designing for other mathematical operations.

To overcome these limitations, it was proposed theoretically to introduce strong nonlocality in the transmission spectrum of a split-ring-resonator array with periodically modulated permittivity in the ring gaps[42]. The Fano-shape leaky-wave resonance due to the interference between the incident and surface waves is sensitive to the oblique incident angle, which supports second derivative and edge detection with a large numerical aperture. To perform the first derivative, the vertical and horizontal mirror symmetry must be broken, which is achieved by adding misplaced metallic wires into the metasurface. The complex design was drastically simplified and experimentally demonstrated in 1D using silicon nanobeams[43] with uniform and two different widths for the second and first derivatives, respectively. Recently, a 2D experimental implementation was also realized, using silicon nanorods embedded in polymethyl methacrylate (PMMA) on a silicon dioxide substrate[45] (Fig. 4c). Due to the leaky guided resonance, the spatial differentiator has a large numerical aperture and can be integrated with either conventional imaging systems, like commercial optical microscope and camera sensor, or metalenses to form a monolithic compound optical system. The latter forms a compact 2D nanophotonic system for edge detection (Fig. 4c).

Metasurfaces are also frequently used with/in computational imaging techniques. On the one hand, postprocessing algorithms in computational imaging provide feasible approaches to optimize the images generated by metalenses. For example, chromatic aberration is strong in metasurfaces due to the local resonances and phase discontinuities. It was proposed that full-color imaging and depth sending of light-field images can be realized by using an array of gallium nitride (GaN) achromatic metalenses with numerous GaN resonators[82]. Also, another work demonstrated that the defocused images from a metalens with cubic phase profile and an extended depth of focus (EDOF) can be recovered using deconvolution to realize full-color metasurface imaging[47]. The method was further developed to simultaneously achieve achromatic and varifocal metasurface imaging[48] where two aligned metalenses with quartic phase profiles are used as inspired by the traditional Alvarez lens (Fig. 4d). By performing spatial Laplacian and finite difference on images from a metalens that incorporates two phase profiles with different in-focus distances, metasurface depth-sensing from the point spread function width was experimentally demonstrated recover[83] (Fig. 4e). On the other hand, metasurface is itself an efficient tool in computation imaging, giving rise to numerous interesting applications like optical steganography, storage, and encryption[84,85]. For example, the polarization sensitivity of nanorod reflective metasurface was proposed to encrypt single-pixel (SP) computational ghost imaging with a strong helicity dependence[86] (Fig. 4f). Also, Zhang et al. proposed another encryption scheme by introducing metasurface-images into the encoding and decoding processes as the keys of SP imaging encryption[87]. Another work demonstrates the realization of covert images with accurate color reproduction by using plasmonic metapixel arrays[88].

Metasurface not only can process information or be optimized by information techniques as mentioned above, but also can be coded by information. In 2014, digital metamaterials were proposed where each unit only takes discrete (binary) values of material parameters[51]. Compared with metamaterials based on analog parameters, it is convenient to form a universal design procedure for digital metamaterials and to incorporate them with existing algorithms and devices for the processing of digital signals. Digital metasurfaces[51] appeared in the same year under similar considerations. For a 1-bit digital metasurface, the 0 and 1 elements are two kinds of meta-atoms with near 0 and π phase responses thanks to their different geometries. In the same work, a programmable digital metasurface was also proposed where each meta-atom can have 0 and π phase responses based on the OFF and ON states of a biased diode connecting two metallic structures (Fig. 4g). Such a device is suitable for information processing in dynamic and complex working conditions and implies novel reconfigurable functionalities. Digital metasurfaces with programmable meta-atoms are called information metasurfaces[53,54]. To date, due to its high demand on the control of each individual meta-atom, the working frequency of information metasurfaces is limited to gigahertz.

Information metasurface is a suitable platform for machine-learning assisted computational imaging since its large number of configurations provide a convenient training set. Using a 2-bit configuration, a real-time metasurface imager has been trained to quickly identify body gestures[49]. Moreover, information metasurface trained with artificial neural networks has been demonstrated to image and recognize people using standard WIFI signals[50]. The real-time tunability of information metasurface introduces another dimension to the code sequences. Space-time coding metasurfaces are such devices that work according to three-dimensional coding matrices (two spatial and one temporal dimension)[89]. Based on it, a new scheme for wireless communication has been demonstrated with high quality and robustness[90]. It is also worth noting that metasurface with carefully designed geometric phase acts as a desired platform for the generation of complex vectorial beams, which can be further used for information transportation and optical communication[91]. Recently, a generic approach was proposed to efficiently generate arbitrary vectorial optical fields based on metasurfaces by exploiting the full-matrix inhomogeneous Jones matrix[92].

The studies mentioned above imply broad potentials of computational and information metasurfaces in smart sensing, imaging, healthcare monitoring, internet of things, wireless power transfer, etc. Towards these applications, higher working frequency, more sophisticated algorithms, and more convenient implementation techniques are still in great demand.

Metasurfaces for quantum technologies

The critically important next step in the flat optics is to combine the physics of metasurfaces with quantum technologies. By coupling quantum emitters to elements of metasurfaces, we can achieve a flexible control of quantum light that can be captured, stored, manipulated, and emitted as a flow of single photons. The corresponding quantum devices can become essential building blocks for realizing secure quantum communication and quantum computing systems. The use of *quantum metasurfaces* with the direct integration of nonclassical sources of light such as single-photon emitters would allow achieving an unprecedented control over emission of photons, thus endowing metadevices with quantum information processing capabilities. High efficiency in such devices requires a collection of photons and control over their emission. In addition, metasurfaces can be employed to mediate *quantum entanglement* between two qubits trapped on a chip and separated by macroscopic distances, by engineering their coherent and dissipative interactions via the metasurface, as was predicted theoretically[55]. Importantly, spatially scalable interaction channels offered by metasurfaces enable robust entanglement[48].

Figures 5(a-e) illustrate several concepts and recent realisations of metasurfaces for manipulating or enhancing quantum effects. Fig. 5(a) presents the recent experiments by Stav et al[56] on the generation of entanglement between the spin and orbital angular momenta of photons[56]. In the first experiment, the photon pairs are splitted by directing one photon through a metasurface and the other photon --to a detector, then detecting the arrival of the other photon. Stav et al[56] measured the single photon that passed through the metasurface and reveal that it acquired an orbital angular momentum and that it became entangled with the spin. In the second experiment, Stav et al[56] passed the single photon pairs through the same metasurface and employ two detectors to show that the photons became entangled, so that the spin of one photon is correlated with the orbital angular momentum of the other photon, and vice versa.

Generation of photon pairs in nonlinear materials enables the creation of non-classical entangled photon states. By integrating metasurface lens with a nonlinear BBO crystal as shown in Fig. 5(b), one can realize a multi-path spontaneous parametric down-conversion photon-pair source which is promising for high-dimensional entanglement and multi-photon state generations. Such a structure was realized by Li et al[59] for metalens 10x10 array who also demonstrated four-photon and six-photon generation with high indistinguishability of photons generated from different metalenses. This metasurface-based quantum photon source is compact, stable, and controllable, indicating a new platform for integrated quantum devices.

Huang et al[60] developed a quantum platform based on diamond with small defects, called nitrogen-vacancy (NV) centres, are known to harbour electron spins that can be manipulated at room temperature, see Fig. 5(c). Each NV centre emits light that provides information about the spin's quantum state. Huang et al[60] fabricated a metasurface on the surface of diamond that acts like metalens to collect photons from a single qubit in diamond and direct them into an optical fibre. This is a first key step in larger efforts to realize compact quantum devices operating at room temperature.

Being integrated with quantum emitters, metasurfaces can create a special meta-platform for quantum photon sources. In the regime of weak coupling, the Purcell enhancement of quantum emitters, or their enhancement of spontaneous emission rates, could enable the development of efficient single-photon sources for quantum optics. From the other hand, we observe the development of the fundamental conceptual and practical advances in realization of multi-photon quantum interference, taking place at subwavelength scale within its short interaction with the metasurface and paving the way to novel types of ultrathin metadevices for the manipulation and measurement of multi-photon quantum entangled photon states.

Unique properties of metasurfaces to manipulate quantum light could find use in a variety of areas, including free-space communications and quantum imaging. A key strength of the system is that it allows photon correlations and quantum state measurements to be harvested using only polarization-insensitive single-photon click detectors. Combining the metasurface with single-photon-sensitive CCD cameras could allow multiple-time-frame images of quantum states. The metasurface is thus analogous to a quantum "camera lens" to allow fast, imaging-based measurements of quantum states.

The use of metasurfaces for quantum optics reveals new opportunities not yet fully explored in both the fields. As an example of the opportunity to enrich both fields of metasurface and quantum optics, in Fig. 5(d) we show the recent experimental demonstration of Zhou et al[46] that a polarization-entangled photon source can be used for switching from "on" to "off" states and back in the optical edge detection realised with optical imaging employing high-efficiency dielectric metasurfaces. This represents a promising direction toward quantum edge detection and image processing with a remarkable signal-to-noise ratio. Another recent work[93] demonstrates first-time generation of photon pairs via spontaneous parametric-down conversion in quantum optical metasurfaces with Mie-like resonances at various wavelengths, enabling flat-optics sources of entangled photons.

Recently suggested spatiotemporally modulated quantum metasurfaces provide a novel flexible platform for generating nonclassical light with designer spatial and spectral shapes[94]. As shown in the conceptual figure Fig. 5(e), they can be employed for on-demand entanglement for free-space communications and for reconfigurable imaging systems. Selective quantum information encoding can be achieved with specific frequency, linear momentum, or orbital angular momentum harmonics. Such novel space-time metasurfaces can provide breakthrough advances in quantum photonics.

As summarized in the recent review[95], special properties of metasurfaces are extremely attractive to manipulate photons and to produce states of nonclassical light, and such important functionalities can be useful in many areas, including free-space communications and quantum imaging. Such metasurface systems can enable complete quantum-state measurements using simple polarization-insensitive single-photon click detectors. Combining the metasurface with single-photon-sensitive charge-coupled device cameras could allow multiple-time-frame images of quantum states. Such metasurfaces can be made similar to quantum cameras allowing fast imaging of quantum states.

In addition to the manipulation of quantum light, metasurfaces may become themselves a novel type of quantum device playing an important role in the field of quantum information and computing, thereby paving the way for numerous practical applications that may include, among others, the development of unbreakable encryptions, as well as opening the door to new possibilities for quantum information systems on a chip.

Perspective and Outlook

It is now widely accepted that photonics plays an important role in our everyday life being closely connected with the progress of technology and key scientific discoveries. Metasurface-empowered flat optics is advancing several grand challenges in photonics. One of those challenges is to realize tunable and switchable metadevices enabling dynamic and active control of the properties of light including its amplitude, phase, wavevector, and polarization. Beam steering with metasurfaces emerged as one of the first important functionalities that immediately opened new applications, also underpinning, and driving new discoveries. Integration of metasurfaces with quantum emitters and creation of multifunctional modulators for light would follow naturally those initial steps.

We believe that further advances in fundamental research in metaphotonics and technological innovations in flat optics will uncover a tremendous potential of metasurfaces making their rapid impact on science, technology, and society. In addition to what we have described above, there are many other areas in physics and applications of metasurfaces that we believe will undergo rapid development in the coming years. Below we mention just a few additional examples of the most recent specific advances in new physics, innovative engineering, and intelligent design of photonic metasurfaces.

New physics with metasurfaces. Metasurfaces suggest the opportunities to go beyond the design limitation by employing subwavelength structure engineering in addition to chemistry-based material arrangements, and thus providing unprecedented innovations in material-based photonic devices and systems. New developments in physics of metasurfaces are driven by the approach to increasing the dimensionality of metamaterials bringing the dimension of "time" into the metasurfaces platform[64], and considering some parameters such as dielectric permittivity ε changing with time in addition to its variation in space, namely $\varepsilon(x, y, z, t)$. In this case, novel physics is associated with causality, so events always move forward in time, being consistent with the second law of thermodynamics. Such differences between space and time provide additional richness to wave-matter interaction in spatiotemporal metamaterials, and such spatiotemporal structures can be used to break the reciprocity without using any biasing magnetic field[96], and temporally varying media exhibit more complex effects such as time-varying polarizabilities.

Metasurfaces have refreshed the considerable interest to the study of special classes of nonradiating modes associated with the so-called bound states in the continuum (BICs) described by embedded eigenvalues[97,98] because they can provide a physical mechanism for trapping electromagnetic energy in small volumes for a long time. A true BIC is a mathematical object with an infinite value of the resonance spectral width, often called the quality factor (Q factor). In practice, BIC can be realized as quasi-BIC, being directly associated with the so-called supercavity mode, where both the Q factor and resonance width become finite. Nevertheless, BIC-inspired resonances of metasurfaces can be employed for many applications such as biosensing, and they can also empower the chiral properties of metasurfaces[99].

Metasurfaces allow to engineer polarization singularities of vectorial electromagnetic fields starting from meta-atoms where polarization singularities may appear already at the level of the Mie theory, and considering various metasurface structures for which both near- and far-field patterns manifest diverse polarization singularities characterized by the integer Poincaré or more general half-integer Hopf indices (topological charges)[63]. Such polarization singularities can provide novel perspectives in the physics of light-matter manipulation for both fundamental physics and practical applications of metasurfaces. A recent example is the demonstration of vortex microlasers generated by a metasurface made of halide perovskite $MAPbBr_3$ by Huang et al.[74]. The authors created a metasurface membrane supporting BICs at the Γ-point of the spectrum associated with vector singularity, and they observed the vortex nature of the laser beams and ultrafast switching. The polarization responses of resonant modes of the metasurface were utilized to induce helical geometric phase shifts to the incident light-generating phase singularities in the far field. Another example of a new physics enabled by metasurfaces is the recent demonstration of a metasurface-based optical chip for the trapping of ensembles of cold atoms with a single incident laser beam. By employing a metasurface, Zhu et al.[100] achieved the trapping of $\sim 10^7$ atoms relevant to quantum sensing, making a step forward for fully integrated cold atom quantum devices by exploiting metasurface optical chips.

Innovative engineering and tunability. Despite many advances, most of the currently demonstrated metasurfaces are static and feature optical responses determined by configurations of meta-atoms set during their fabrication. Significant challenges are to design and realize active metasurfaces with pixel-level programmability and addressability, given the intrinsic impediments to impose active responses and gain accurate control over the individual optical elements at the nanoscale. Metasurfaces with spatially arranged meta-atoms can directly change light properties such as phase, amplitude, and polarization. If each meta-atom serves as a pixel, and it can be controlled independently, it becomes possible to realize addressable and programmable metasurfaces at the subwavelength pixel level. Dynamic configurations investigated so far by using controlled constituent materials or geometrical parameters often exhibit specific limitations and reduced reconfigurability. Very recently, Meng et al.[65] combined a plasmonic metasurface with a thin-film piezoelectric MEMS and have developed an electrically driven dynamic MEMS-metasurface platform for controlling phase and amplitude of the reflected light by finely actuating the MEMS mirror. They have demonstrated MEMS-metasurface components for polarization-independent beam steering and focusing with high modulation efficiencies (~ 50%) and fast responses (< 0.4 ms).

Tunability of metasurfaces is a critically important feature required for many applications. It is often achieved in hybrid systems when metasurfaces are combined with other materials such as liquid crystals or phase-change material $Ge_2Sb_2Te_5$ (known as GST) embedded into meta-atom arrays for active and non-volatile tuning of properties of light. As a recent example, Abdollahramezani et al.[101] designed a meta-atom, which selectively controls the hybrid plasmonic-photonic resonances of reconfigurable metasurfaces via the dynamic change of GST optical constants. They have demonstrated two tunable metasurfaces that control the amplitude (with modulation depth ≈80%) or phase (with tunability >230°) of incident light for high contrast switching and efficient beam deflection.

Advanced design strategies. Recent advancements in machine learning and artificial intelligence will contribute to reshape substantially some major areas of photonics where metasurfaces may play a more and more important role. Indeed, to develop metasurfaces with specific properties and functionalities, we need novel design strategies and approaches based on advanced computational techniques. Machine learning is emerging as a special subfield of artificial intelligence[102] that is advancing many areas of science and engineering, and it is expected that the methods of machine learning and deep learning will be useful for sophisticated designs of smartphones, robotic systems, and self-driving cars.

Nanophotonics involves different platforms and designs which require careful engineering and optimisation of the properties of meta-atoms and their arrays, especially for creating hybrid systems integrated with 2D materials and quantum emitters. Unconventional optical designs can be discovered via machine learning thus advancing imaging, sensing, and other functionalities for on-chip circuitry. Many recent studies are devoted to photonic design approaches and emerging material platforms showcasing machine-learning-assisted optimization for intelligent metasurface designs.

The practical realization of efficient metasurfaces is a complex problem due to the multitude of constraints implying large optimization spaces. Recently, Kudyshev et al[61] suggested the topology optimization method combined with deep learning algorithms, and they employed this knowledge to optimize the design of a thermal emitter metasurface with high-efficiency thermal emission reshaping. They demonstrated substantial improvement of computational time (almost 5000 times faster) and final devices' efficiencies (98%). A global optimization allows uncovering efficient topology-optimized metasurfaces operating across a range of parameters, with metasurfaces operating across a range of wavelengths and angles as a model system. Jiang and Fan[62] demonstrated that devices produced from the trained generative network have efficiencies comparable to or better than the best devices produced by adjoint-based topology optimization while requiring less computational costs.

While metasurfaces have been intensively studied and enjoyed rapid development in the past decade, several significant challenges still exist for practical and end-specific utilizations. Set aside common challenges like loss and tunability mentioned above, when it comes to the optical region, fabrication becomes a tricky problem for many accuracy-required structures such as BIC-empowered metasurfaces, and it also becomes harder to modulate metasurfaces, because the properties of common materials can rarely be tuned in billions or trillions per second. With emerging materials, new physics and advanced nanofabrication techniques, those challenges may be bypassed. We anticipate new insights being delivered by merging the concepts from several fields exploring time-varying photonics and creating new types of hybrid and multi-layer systems governed by the concepts of flat optics and metamaterial-inspired subwavelength engineering. We expect that the future research in metasurfaces will significantly broaden the horizons of photonics and offer new perspectives for metaphotonics, leading to novel applications beyond our current imagination.

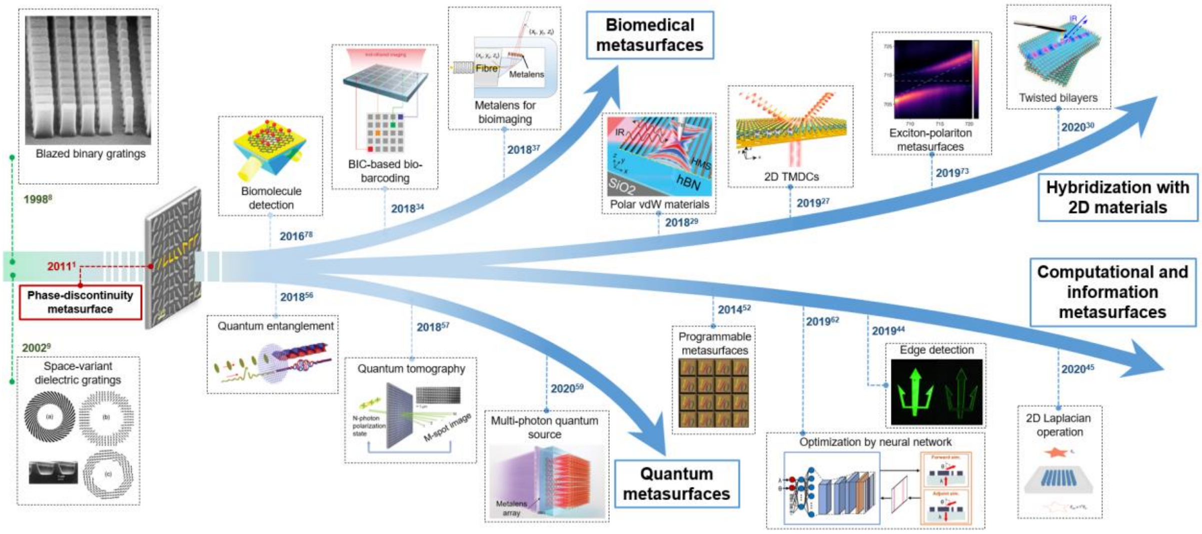

Figure 1. Major milestones and selected key directions for the research on metasurfaces. Notations are BIC, bound state in the continuum; 2D, two-dimensional; TMDCs, transition metal dichalcogenides; vdW, van der Waals. And hBN, hexagonal boron nitride. Adapted with permission from refs. 1, 8, 9, 27, 29, 30, 34, 37, 44, 45, 52, 56, 57, 59, 62, 73, and 78.

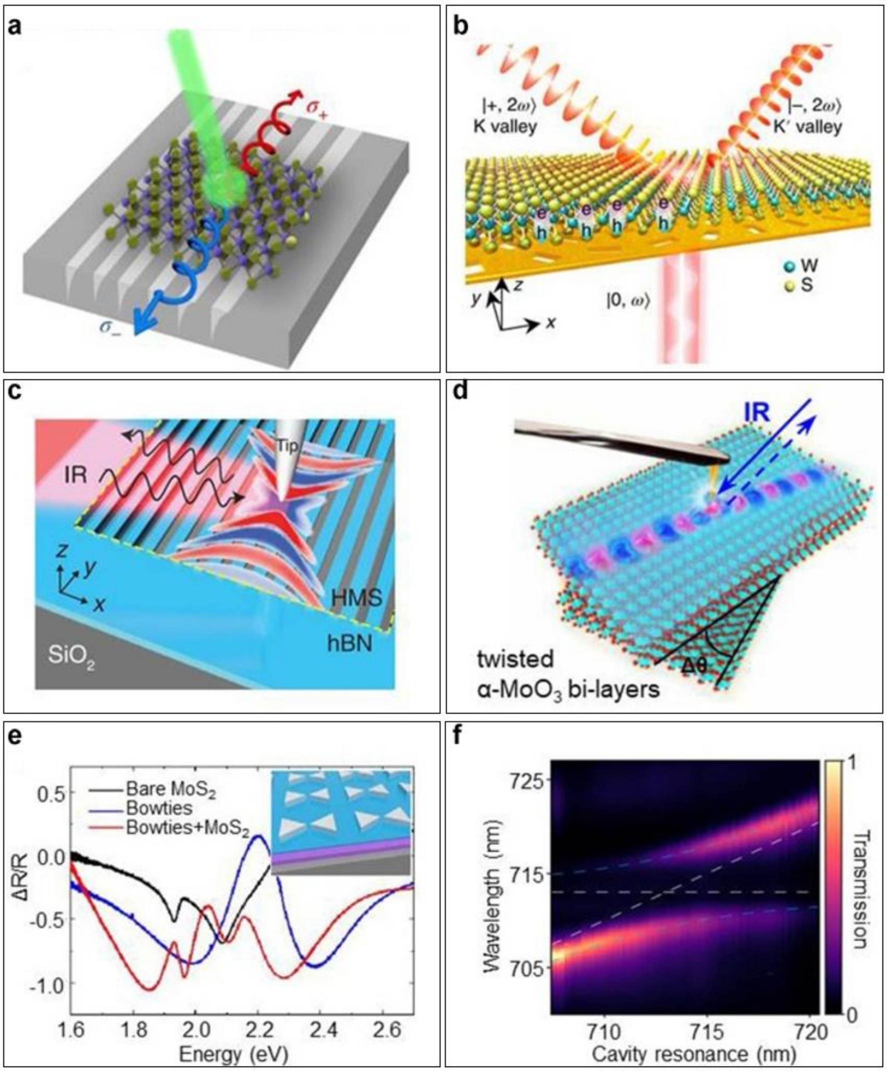

Figure 2. Hybridization of metasurfaces with 2D materials. a, Metasurface made of an array of asymmetric grooves directs the valley excitons. Adapted with permission from ref. 24. Copyright 2019 Springer Nature. **b,** Geometric phase metasurface steers nonlinear chiral valley photons. Adapted with permission from ref. 27. Copyright 2019 Springer Nature. **c,** Grating hBN metasurface supports in-plane propagation of hyperbolic phonon polaritons. Adapted with permission from ref. 29. Copyright 2018 AAAS. **d,** Twisted α-MoO_3 bilayers facilitates the extreme dispersion engineering originally sustained in moiré hyperbolic metasurfaces. Adapted with permission from ref. 30. Copyright 2020 Springer Nature. **e,** Bowtie-MoS_2 hybrid system features intermediate light-matter interaction manifested via Fano resonance. Adapted with permission from ref. 72. Copyright 2015 American Chemical Society. **f,** Plasmonic -WSe_2 system supports strong light-matter interaction revealed by the avoided anticrossing in the transmission spectra. Adapted with permission from ref. 73. Copyright 2019 American Chemical Society.

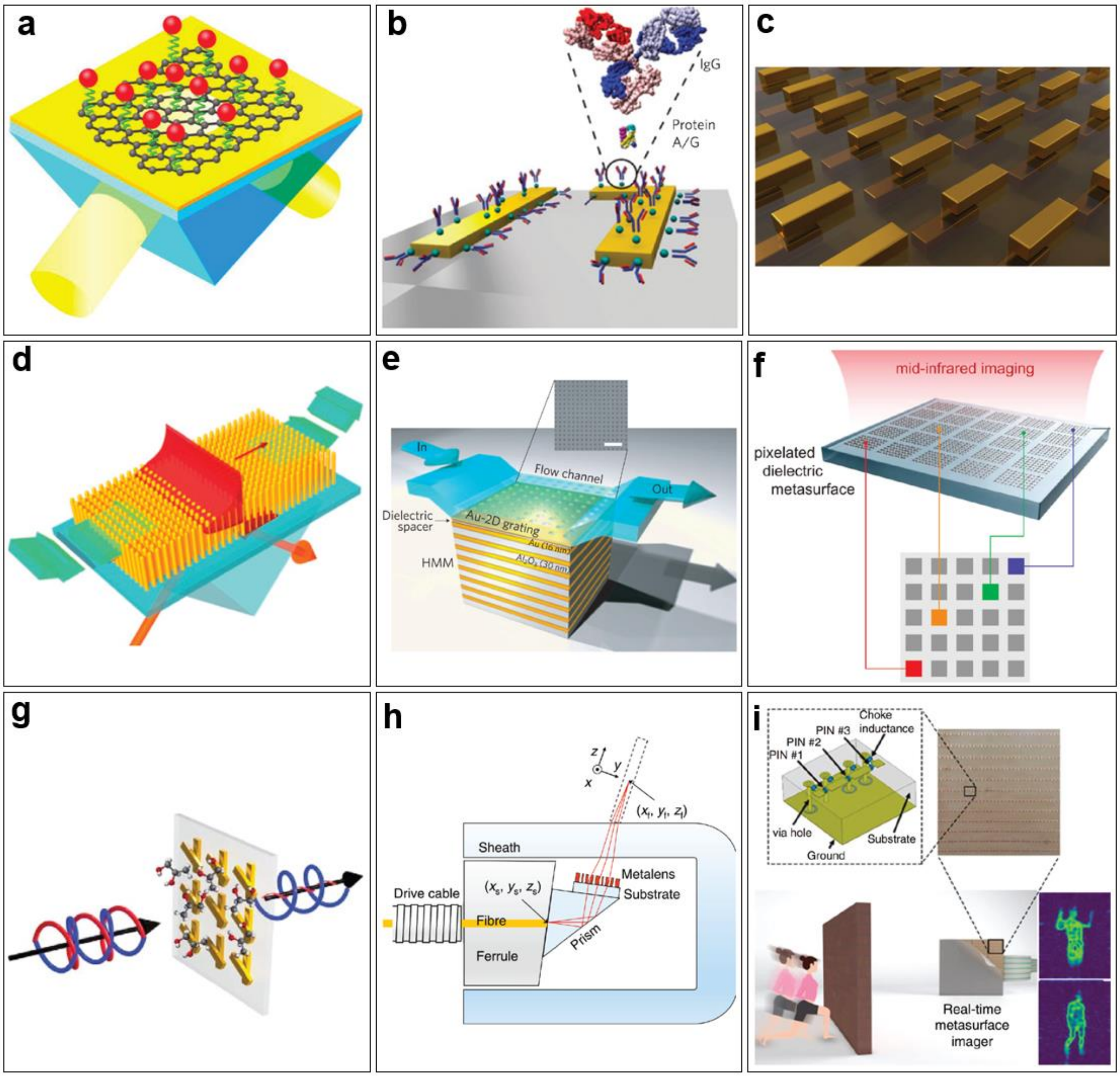

Figure 3. Metasurfaces for biomedical applications. a, Metasurface consisting of nanoparticle-enhanced graphene-gold multilayers for detection of single-stranded DNA. Adapted with permission from ref. 78. Copyright 2015 WILEY-VCH Verlag GmbH & Co. KGaA, Weinheim. **b,** Metasurface biosensor based on Fano resonance for detection of protein. Adapted with permission from ref. 32. Copyright 2011 Springer Nature. **c,** Metasurface based on symmetry-breaking-induced plasmonic exceptional point for immune-assay nanoscale sensing. Adapted with permission from ref. 33. Copyright 2020 Springer Nature. **d,** Hyperbolic metamaterial consisting of parallel Au nanorod array for detection of biotin. Adapted with permission from ref. 79. Copyright 2009 Springer Nature. **e,** Metallic diffraction grating-coupled hyperbolic metamaterial biosensor with a fluid flow channel. Adapted with permission from ref. 80. Copyright 2016 Springer Nature. **f,** Pixelated metasurface composed of a two-dimensional array of high-Q resonant metapixels for molecular fingerprint detection. Adapted with permission from ref. 34. Copyright 2018 AAAS. **g,** Chiral metasurface consisting of twisted Au nanorods for enhanced chiral biomolecular sensing. Adapted with permission from ref. 36. Copyright 2017 Springer Nature. **h,** Metalens endoscope for optical coherence tomography. Adapted with permission from ref. 37. Copyright 2018 Springer Nature. **i,** Machine-learning reprogrammable metasurface for microwave imaging of a moving person behind a wall. Adapted with permission from ref. 49. Copyright 2019 Springer Nature.

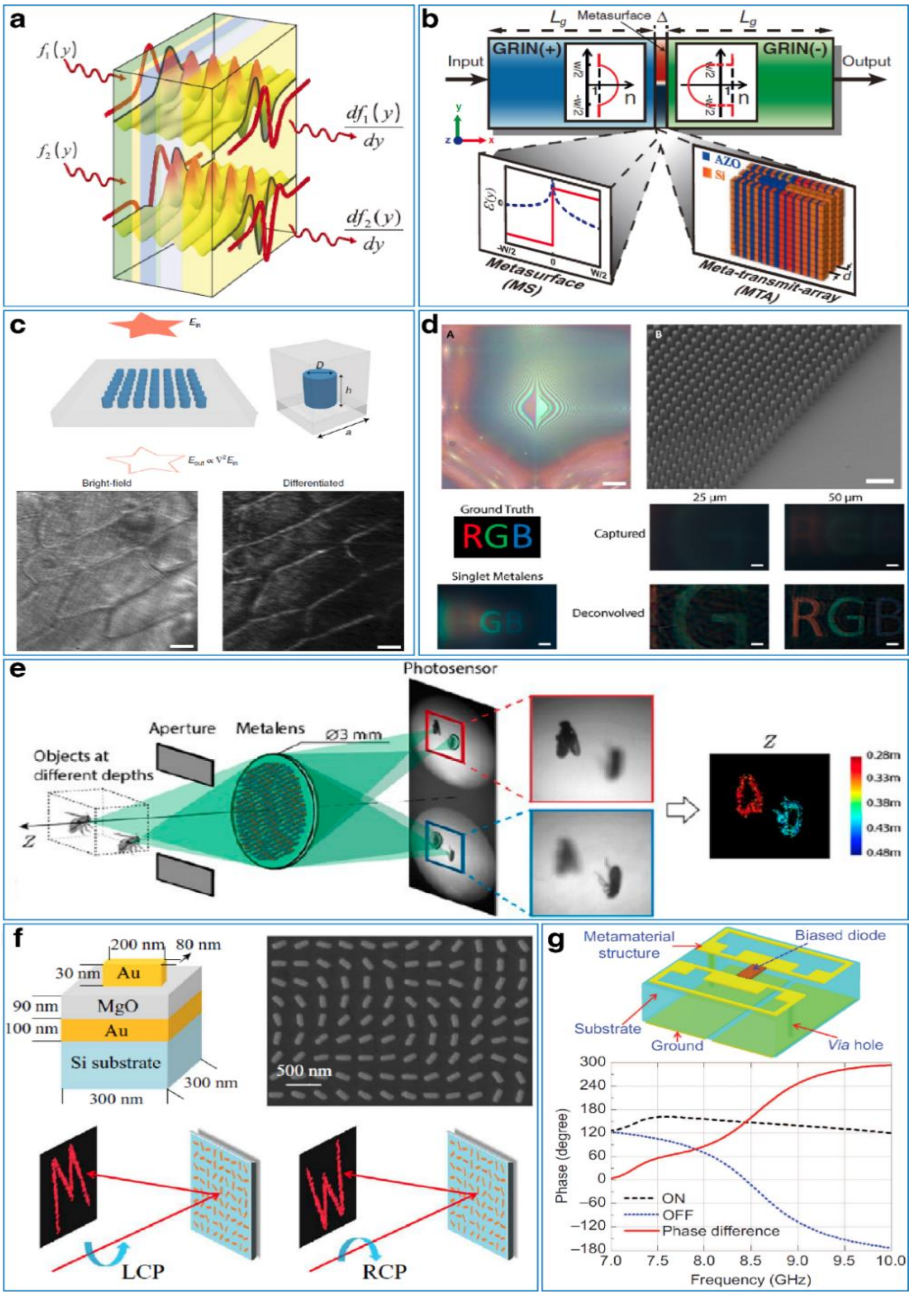

Figure 4. Computational and information metasurfaces. a, Performing spatial differentiation on light fields. Adapted with permission from ref. 38. Copyright 2014 AAAS. **b,** Structure that performs analog computation: two graded-index slabs with a conceptual metasurface or a meta-transmit-array. Adapted with permission from ref. 38. Copyright 2014 AAAS. **c,** Using its leaky guided resonance, a dielectric photonic crystal slab can perform two-dimensional (2D) Laplacian operation for edge detection (upper). It can be combined with metalens to form a monolithic compound system that processes the image of onion cells (lower). Adapted with permission from ref. 45. Copyright 2020 Springer Nature. **d,** Achromatic and varifocal imaging with a continuously tunable extended depth of focus using two quartic metasurfaces. Adapted with permission from ref. 48. Copyright 2020 American Chemical Society. **e,** Depth sensing using a metalens incorporated with two different in-focus distances. Adapted with permission from ref. 83. Copyright 2019 National Academy of Sciences. **f,** Helicity dependent computational ghost imaging with metasurface. Adapted with permission from ref. 86. Copyright 2017 AAAS. **g,** Structure and phase response of the meta-atom in a programmable digital metasurface or information metasurface. Adapted with permission from ref. 52. Copyright 2014 Springer Nature.

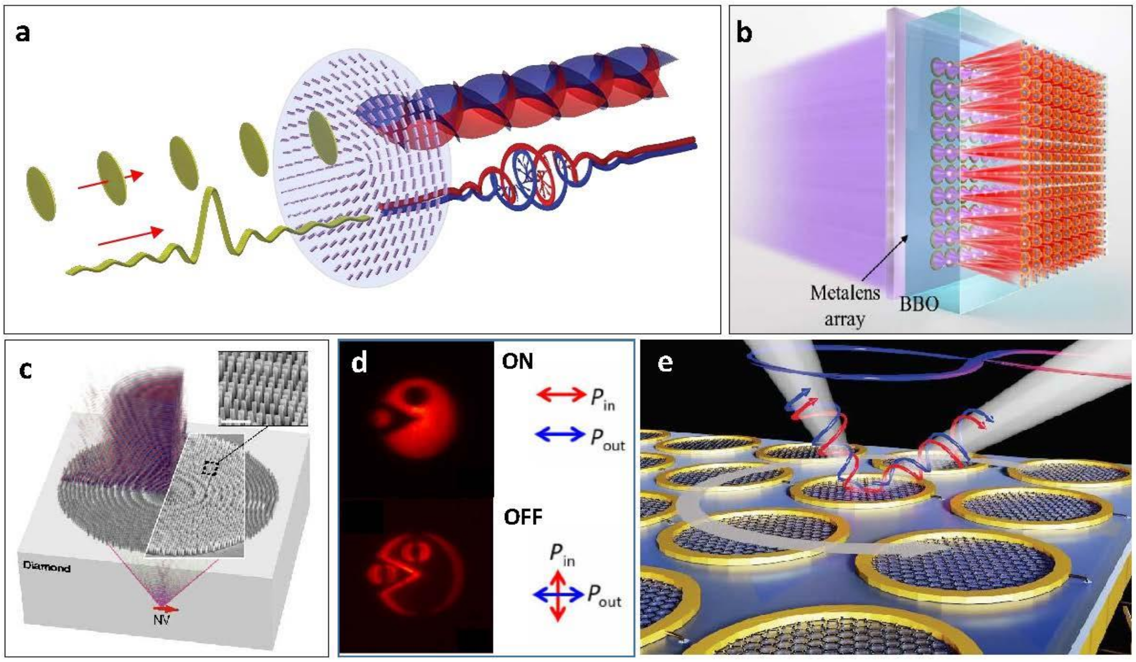

Fig 5. Metasurfaces for quantum technologies. a, Quantum entanglement of the spin and orbital angular momentum. Adapted with permission from ref. 56. Copyright 2018 AAAS. **b,** Metalens multi-photon quantum source. Adapted with permission from ref. 59. Copyright 2020 AAAS. **c,** Diamond metalens to collect and collimate emission of an individual NV centre. Adapted with permission from ref. 60. Copyright 2019 Springer Nature. **d,** Demonstration of switchable edge detection**.** The image of the object comprising the separated LCP and RCP components, which is the OFF state of the edge detection mode. The image reveals edges for the ON state of the edge detection mode. Adapted with permission from ref. 46. Copyright 2020 AAAS. **e,** Conceptual representation of a space-time quantum metasurface. A spatiotemporal spinning modulation of graphene nanostructures generates entangled vortex photon pairs out of the quantum vacuum. Adapted with permission from ref. 94. Copyright 2021 D.A.R. Dalvit.

References

(1) Yu, N.; Genevet, P.; Kats, M. A.; Aieta, F.; Tetienne, J.-P.; Capasso, F.; Gaburro, Z. Light Propagation with Phase Discontinuities: Generalized Laws of Reflection and Refraction. *Science* **2011**, *334* (6054), 333–337. https://doi.org/10.1126/science.1210713.

(2) Kildishev, A. V.; Boltasseva, A.; Shalaev, V. M. Planar Photonics with Metasurfaces. *Science* **2013**, *339* (6125), 1232009. https://doi.org/10.1126/science.1232009.

(3) Yu, N.; Capasso, F. Flat Optics with Designer Metasurfaces. *Nature Materials* **2014**, *13* (2), 139–150. https://doi.org/10.1038/nmat3839.

(4) Arbabi, A.; Horie, Y.; Bagheri, M.; Faraon, A. Dielectric Metasurfaces for Complete Control of Phase and Polarization with Subwavelength Spatial Resolution and High Transmission. *Nature Nanotechnology* **2015**, *10* (11), 937–943. https://doi.org/10.1038/nnano.2015.186.

(5) Sun, S.; He, Q.; Xiao, S.; Xu, Q.; Li, X.; Zhou, L. Gradient-Index Meta-Surfaces as a Bridge Linking Propagating Waves and Surface Waves. *Nature Materials* **2012**, *11* (5), 426–431. https://doi.org/10.1038/nmat3292.

(6) Sun, S.; Yang, K.-Y.; Wang, C.-M.; Juan, T.-K.; Chen, W. T.; Liao, C. Y.; He, Q.; Xiao, S.; Kung, W.-T.; Guo, G.-Y.; Zhou, L.; Tsai, D. P. High-Efficiency Broadband Anomalous Reflection by Gradient Meta-Surfaces. *Nano Lett.* **2012**, *12* (12), 6223–6229. https://doi.org/10.1021/nl3032668.

(7) Pfeiffer, C.; Grbic, A. Metamaterial Huygens' Surfaces: Tailoring Wave Fronts with Reflectionless Sheets. *Phys. Rev. Lett.* **2013**, *110* (19), 197401. https://doi.org/10.1103/PhysRevLett.110.197401.

(8) Lalanne, P.; Astilean, S.; Chavel, P.; Cambril, E.; Launois, H. Blazed Binary Subwavelength Gratings with Efficiencies Larger than Those of Conventional Échelette Gratings. *Opt. Lett.* **1998**, *23* (14), 1081. https://doi.org/10.1364/OL.23.001081.

(9) Bomzon, Z.; Biener, G.; Kleiner, V.; Hasman, E. Radially and Azimuthally Polarized Beams Generated by Space-Variant Dielectric Subwavelength Gratings. *Opt. Lett.* **2002**, *27* (5), 285. https://doi.org/10.1364/OL.27.000285.

(10) Xu, H.-X.; Hu, G.; Han, L.; Jiang, M.; Huang, Y.; Li, Y.; Yang, X.; Ling, X.; Chen, L.; Zhao, J.; Qiu, C.-W. Chirality-Assisted High-Efficiency Metasurfaces with Independent Control of Phase, Amplitude, and Polarization. *Advanced Optical Materials* **2019**, *7* (4), 1801479. https://doi.org/10.1002/adom.201801479.

(11) Lin, D.; Fan, P.; Hasman, E.; Brongersma, M. L. Dielectric Gradient Metasurface Optical Elements. *Science* **2014**, *345* (6194), 298–302. https://doi.org/10.1126/science.1253213.

(12) Dai, Z.; Hu, G.; Ou, Q.; Zhang, L.; Xia, F.; Garcia-Vidal, F. J.; Qiu, C.-W.; Bao, Q. Artificial Metaphotonics Born Naturally in Two Dimensions. *Chem. Rev.* **2020**, *120* (13), 6197–6246. https://doi.org/10.1021/acs.chemrev.9b00592.

(13) Khorasaninejad, M.; Chen, W. T.; Devlin, R. C.; Oh, J.; Zhu, A. Y.; Capasso, F. Metalenses at Visible Wavelengths: Diffraction-Limited Focusing and Subwavelength Resolution Imaging. *Science* **2016**, *352* (6290), 1190–1194. https://doi.org/10.1126/science.aaf6644.

(14) Chen, W. T.; Yang, K.-Y.; Wang, C.-M.; Huang, Y.-W.; Sun, G.; Chiang, I.-D.; Liao, C. Y.; Hsu, W.-L.; Lin, H. T.; Sun, S.; Zhou, L.; Liu, A. Q.; Tsai, D. P. High-Efficiency Broadband Meta-Hologram with Polarization-Controlled Dual Images. *Nano Lett.* **2014**, *14* (1), 225–230. https://doi.org/10.1021/nl403811d.

(15) Zheng, G.; Mühlenbernd, H.; Kenney, M.; Li, G.; Zentgraf, T.; Zhang, S. Metasurface Holograms Reaching 80% Efficiency. *Nature Nanotechnology* **2015**, *10* (4), 308–312. https://doi.org/10.1038/nnano.2015.2.

(16) Huang, Y.-W.; Chen, W. T.; Tsai, W.-Y.; Wu, P. C.; Wang, C.-M.; Sun, G.; Tsai, D. P. Aluminum Plasmonic Multicolor Meta-Hologram. *Nano Lett.* **2015**, *15* (5), 3122–3127. https://doi.org/10.1021/acs.nanolett.5b00184.
(17) Tymchenko, M.; Gomez-Diaz, J. S.; Lee, J.; Nookala, N.; Belkin, M. A.; Alù, A. Gradient Nonlinear Pancharatnam-Berry Metasurfaces. *Phys. Rev. Lett.* **2015**, *115* (20), 207403. https://doi.org/10.1103/PhysRevLett.115.207403.
(18) Li, G.; Chen, S.; Pholchai, N.; Reineke, B.; Wong, P. W. H.; Pun, E. Y. B.; Cheah, K. W.; Zentgraf, T.; Zhang, S. Continuous Control of the Nonlinearity Phase for Harmonic Generations. *Nature Materials* **2015**, *14* (6), 607–612. https://doi.org/10.1038/nmat4267.
(19) Wu, P. C.; Tsai, W.-Y.; Chen, W. T.; Huang, Y.-W.; Chen, T.-Y.; Chen, J.-W.; Liao, C. Y.; Chu, C. H.; Sun, G.; Tsai, D. P. Versatile Polarization Generation with an Aluminum Plasmonic Metasurface. *Nano Lett.* **2017**, *17* (1), 445–452. https://doi.org/10.1021/acs.nanolett.6b04446.
(20) Chen, H.-T.; Taylor, A. J.; Yu, N. A Review of Metasurfaces: Physics and Applications. *Rep. Prog. Phys.* **2016**, *79* (7), 076401. https://doi.org/10.1088/0034-4885/79/7/076401.
(21) He, Q.; Sun, S.; Xiao, S.; Zhou, L. High-Efficiency Metasurfaces: Principles, Realizations, and Applications. *Advanced Optical Materials* **2018**, *6* (19), 1800415. https://doi.org/10.1002/adom.201800415.
(22) Sun, S.; He, Q.; Hao, J.; Xiao, S.; Zhou, L. Electromagnetic Metasurfaces: Physics and Applications. *Advances in Optics and Photonics* **2019**, *11*, 380. https://doi.org/10.1364/AOP.11.000380.
(23) Ermolaev, G. A.; Grudinin, D. V.; Stebunov, Y. V.; Voronin, K. V.; Kravets, V. G.; Duan, J.; Mazitov, A. B.; Tselikov, G. I.; Bylinkin, A.; Yakubovsky, D. I.; Novikov, S. M.; Baranov, D. G.; Nikitin, A. Y.; Kruglov, I. A.; Shegai, T.; Alonso-González, P.; Grigorenko, A. N.; Arsenin, A. V.; Novoselov, K. S.; Volkov, V. S. Giant Optical Anisotropy in Transition Metal Dichalcogenides for Next-Generation Photonics. *Nature Communications* **2021**, *12* (1), 854. https://doi.org/10.1038/s41467-021-21139-x.
(24) Sun, L.; Wang, C.-Y.; Krasnok, A.; Choi, J.; Shi, J.; Gomez-Diaz, J. S.; Zepeda, A.; Gwo, S.; Shih, C.-K.; Alù, A.; Li, X. Separation of Valley Excitons in a MoS 2 Monolayer Using a Subwavelength Asymmetric Groove Array. *Nature Photonics* **2019**, *13* (3), 180–184. https://doi.org/10.1038/s41566-019-0348-z.
(25) Gong, S.-H.; Alpeggiani, F.; Sciacca, B.; Garnett, E. C.; Kuipers, L. Nanoscale Chiral Valley-Photon Interface through Optical Spin-Orbit Coupling. *Science* **2018**, *359* (6374), 443–447. https://doi.org/10.1126/science.aan8010.
(26) van de Groep, J.; Song, J.-H.; Celano, U.; Li, Q.; Kik, P. G.; Brongersma, M. L. Exciton Resonance Tuning of an Atomically Thin Lens. *Nat. Photonics* **2020**, *14* (7), 426–430. https://doi.org/10.1038/s41566-020-0624-y.
(27) Hu, G.; Hong, X.; Wang, K.; Wu, J.; Xu, H.-X.; Zhao, W.; Liu, W.; Zhang, S.; Garcia-Vidal, F.; Wang, B.; Lu, P.; Qiu, C.-W. Coherent Steering of Nonlinear Chiral Valley Photons with a Synthetic Au–WS2 Metasurface. *Nat. Photonics* **2019**, *13* (7), 467–472. https://doi.org/10.1038/s41566-019-0399-1.
(28) Verre, R.; Baranov, D. G.; Munkhbat, B.; Cuadra, J.; Käll, M.; Shegai, T. Transition Metal Dichalcogenide Nanodisks as High-Index Dielectric Mie Nanoresonators. *Nature Nanotechnology* **2019**, *14* (7), 679–683. https://doi.org/10.1038/s41565-019-0442-x.
(29) Li, P.; Dolado, I.; Alfaro-Mozaz, F. J.; Casanova, F.; Hueso, L. E.; Liu, S.; Edgar, J. H.; Nikitin, A. Y.; Vélez, S.; Hillenbrand, R. Infrared Hyperbolic Metasurface Based on Nanostructured van Der Waals Materials. *Science* **2018**, *359* (6378), 892–896. https://doi.org/10.1126/science.aaq1704.

(30) Hu, G.; Ou, Q.; Si, G.; Wu, Y.; Wu, J.; Dai, Z.; Krasnok, A.; Mazor, Y.; Zhang, Q.; Bao, Q.; Qiu, C.-W.; Alù, A. Topological Polaritons and Photonic Magic Angles in Twisted α-MoO 3 Bilayers. *Nature* **2020**, *582* (7811), 209–213. https://doi.org/10.1038/s41586-020-2359-9.
(31) Li, P.; Hu, G.; Dolado, I.; Tymchenko, M.; Qiu, C.-W.; Alfaro-Mozaz, F. J.; Casanova, F.; Hueso, L. E.; Liu, S.; Edgar, J. H.; Vélez, S.; Alu, A.; Hillenbrand, R. Collective Near-Field Coupling and Nonlocal Phenomena in Infrared-Phononic Metasurfaces for Nano-Light Canalization. *Nature Communications* **2020**, *11* (1), 3663. https://doi.org/10.1038/s41467-020-17425-9.
(32) Wu, C.; Khanikaev, A.; Adato, R.; Arju, N.; Yanik, A.; Altug, H.; Shvets, G. Fano-Resonant Asymmetric Metamaterials for Ultrasensitive Spectroscopy and Identification of Molecular Monolayers. *Nature materials* **2011**, *11*, 69–75. https://doi.org/10.1038/nmat3161.
(33) Park, J.-H.; Ndao, A.; Cai, W.; Hsu, L.; Kodigala, A.; Lepetit, T.; Lo, Y.-H.; Kanté, B. Symmetry-Breaking-Induced Plasmonic Exceptional Points and Nanoscale Sensing. *Nature Physics* **2020**, *16* (4), 462–468. https://doi.org/10.1038/s41567-020-0796-x.
(34) Tittl, A.; Leitis, A.; Liu, M.; Yesilkoy, F.; Choi, D.-Y.; Neshev, D. N.; Kivshar, Y. S.; Altug, H. Imaging-Based Molecular Barcoding with Pixelated Dielectric Metasurfaces. *Science* **2018**, *360* (6393), 1105–1109. https://doi.org/10.1126/science.aas9768.
(35) Yesilkoy, F.; Arvelo, E. R.; Jahani, Y.; Liu, M.; Tittl, A.; Cevher, V.; Kivshar, Y.; Altug, H. Ultrasensitive Hyperspectral Imaging and Biodetection Enabled by Dielectric Metasurfaces. *Nat. Photonics* **2019**, *13* (6), 390–396. https://doi.org/10.1038/s41566-019-0394-6.
(36) Zhao, Y.; Askarpour, A. N.; Sun, L.; Shi, J.; Li, X.; Alù, A. Chirality Detection of Enantiomers Using Twisted Optical Metamaterials. *Nature Communications* **2017**, *8* (1), 14180. https://doi.org/10.1038/ncomms14180.
(37) Pahlevaninezhad, H.; Khorasaninejad, M.; Huang, Y.-W.; Shi, Z.; Hariri, L. P.; Adams, D. C.; Ding, V.; Zhu, A.; Qiu, C.-W.; Capasso, F.; Suter, M. J. Nano-Optic Endoscope for High-Resolution Optical Coherence Tomography in Vivo. *Nature Photonics* **2018**, *12* (9), 540–547. https://doi.org/10.1038/s41566-018-0224-2.
(38) Silva, A.; Monticone, F.; Castaldi, G.; Galdi, V.; Alù, A.; Engheta, N. Performing Mathematical Operations with Metamaterials. *Science* **2014**, *343* (6167), 160–163. https://doi.org/10.1126/science.1242818.
(39) Pors, A.; Nielsen, M. G.; Bozhevolnyi, S. I. Analog Computing Using Reflective Plasmonic Metasurfaces. *Nano Lett.* **2015**, *15* (1), 791–797. https://doi.org/10.1021/nl5047297.
(40) Zhu, T.; Zhou, Y.; Lou, Y.; Ye, H.; Qiu, M.; Ruan, Z.; Fan, S. Plasmonic Computing of Spatial Differentiation. *Nature Communications* **2017**, *8* (1), 15391. https://doi.org/10.1038/ncomms15391.
(41) Guo, C.; Xiao, M.; Minkov, M.; Shi, Y.; Fan, S. Photonic Crystal Slab Laplace Operator for Image Differentiation. *Optica* **2018**, *5* (3), 251. https://doi.org/10.1364/OPTICA.5.000251.
(42) Kwon, H.; Sounas, D.; Cordaro, A.; Polman, A.; Alù, A. Nonlocal Metasurfaces for Optical Signal Processing. *Phys. Rev. Lett.* **2018**, *121* (17), 173004. https://doi.org/10.1103/PhysRevLett.121.173004.
(43) Cordaro, A.; Kwon, H.; Sounas, D.; Koenderink, A. F.; Alù, A.; Polman, A. High-Index Dielectric Metasurfaces Performing Mathematical Operations. *Nano Lett.* **2019**, *19* (12), 8418–8423. https://doi.org/10.1021/acs.nanolett.9b02477.
(44) Zhou, J.; Qian, H.; Chen, C.-F.; Zhao, J.; Li, G.; Wu, Q.; Luo, H.; Wen, S.; Liu, Z. Optical Edge Detection Based on High-Efficiency Dielectric Metasurface. *PNAS* **2019**, *116* (23), 11137–11140. https://doi.org/10.1073/pnas.1820636116.

(45) Zhou, Y.; Zheng, H.; Kravchenko, I. I.; Valentine, J. Flat Optics for Image Differentiation. *Nature Photonics* **2020**, *14* (5), 316–323. https://doi.org/10.1038/s41566-020-0591-3.
(46) Zhou, J.; Liu, S.; Qian, H.; Li, Y.; Luo, H.; Wen, S.; Zhou, Z.; Guo, G.; Shi, B.; Liu, Z. Metasurface Enabled Quantum Edge Detection. *Science Advances* **2020**, *6* (51), eabc4385. https://doi.org/10.1126/sciadv.abc4385.
(47) Colburn, S.; Zhan, A.; Majumdar, A. Metasurface Optics for Full-Color Computational Imaging. *Science Advances* **2018**, *4* (2), eaar2114. https://doi.org/10.1126/sciadv.aar2114.
(48) Colburn, S.; Majumdar, A. Simultaneous Achromatic and Varifocal Imaging with Quartic Metasurfaces in the Visible. *ACS Photonics* **2020**, *7* (1), 120–127. https://doi.org/10.1021/acsphotonics.9b01216.
(49) Li, L.; Ruan, H.; Liu, C.; Li, Y.; Shuang, Y.; Alù, A.; Qiu, C.-W.; Cui, T. J. Machine-Learning Reprogrammable Metasurface Imager. *Nature Communications* **2019**, *10* (1), 1082. https://doi.org/10.1038/s41467-019-09103-2.
(50) Li, L.; Shuang, Y.; Ma, Q.; Li, H.; Zhao, H.; Wei, M.; Liu, C.; Hao, C.; Qiu, C.-W.; Cui, T. J. Intelligent Metasurface Imager and Recognizer. *Light: Science & Applications* **2019**, *8* (1), 97. https://doi.org/10.1038/s41377-019-0209-z.
(51) Della Giovampaola, C.; Engheta, N. Digital Metamaterials. *Nature Materials* **2014**, *13* (12), 1115–1121. https://doi.org/10.1038/nmat4082.
(52) Cui, T. J.; Qi, M. Q.; Wan, X.; Zhao, J.; Cheng, Q. Coding Metamaterials, Digital Metamaterials and Programmable Metamaterials. *Light: Science & Applications* **2014**, *3* (10), e218–e218. https://doi.org/10.1038/lsa.2014.99.
(53) Jun Cui, T.; Liu, S.; Zhang, L. Information Metamaterials and Metasurfaces. *Journal of Materials Chemistry C* **2017**, *5* (15), 3644–3668. https://doi.org/10.1039/C7TC00548B.
(54) Li, L.; Cui, T. J. Information Metamaterials – from Effective Media to Real-Time Information Processing Systems. *Nanophotonics* **2019**, *8* (5), 703–724. https://doi.org/10.1515/nanoph-2019-0006.
(55) Jha, P. K.; Shitrit, N.; Kim, J.; Ren, X.; Wang, Y.; Zhang, X. Metasurface-Mediated Quantum Entanglement. *ACS Photonics* **2018**, *5* (3), 971–976. https://doi.org/10.1021/acsphotonics.7b01241.
(56) Stav, T.; Faerman, A.; Maguid, E.; Oren, D.; Kleiner, V.; Hasman, E.; Segev, M. Quantum Entanglement of the Spin and Orbital Angular Momentum of Photons Using Metamaterials. *Science* **2018**, *361* (6407), 1101–1104. https://doi.org/10.1126/science.aat9042.
(57) Wang, K.; Titchener, J. G.; Kruk, S. S.; Xu, L.; Chung, H.-P.; Parry, M.; Kravchenko, I. I.; Chen, Y.-H.; Solntsev, A. S.; Kivshar, Y. S.; Neshev, D. N.; Sukhorukov, A. A. Quantum Metasurface for Multiphoton Interference and State Reconstruction. *Science* **2018**, *361* (6407), 1104–1108. https://doi.org/10.1126/science.aat8196.
(58) Bekenstein, R.; Pikovski, I.; Pichler, H.; Shahmoon, E.; Yelin, S. F.; Lukin, M. D. Quantum Metasurfaces with Atom Arrays. *Nature Physics* **2020**, *16* (6), 676–681. https://doi.org/10.1038/s41567-020-0845-5.
(59) Li, L.; Liu, Z.; Ren, X.; Wang, S.; Su, V.-C.; Chen, M.-K.; Chu, C. H.; Kuo, H. Y.; Liu, B.; Zang, W.; Guo, G.; Zhang, L.; Wang, Z.; Zhu, S.; Tsai, D. P. Metalens-Array–Based High-Dimensional and Multiphoton Quantum Source. *Science* **2020**, *368* (6498), 1487–1490. https://doi.org/10.1126/science.aba9779.
(60) Huang, T.-Y.; Grote, R. R.; Mann, S. A.; Hopper, D. A.; Exarhos, A. L.; Lopez, G. G.; Kaighn, G. R.; Garnett, E. C.; Bassett, L. C. A Monolithic Immersion Metalens for Imaging Solid-State Quantum Emitters. *Nature Communications* **2019**, *10* (1), 2392. https://doi.org/10.1038/s41467-019-10238-5.

(61) Kudyshev, Z. A.; Kildishev, A. V.; Shalaev, V. M.; Boltasseva, A. Machine-Learning-Assisted Metasurface Design for High-Efficiency Thermal Emitter Optimization. *Applied Physics Reviews* **2020**, *7* (2), 021407. https://doi.org/10.1063/1.5134792.
(62) Jiang, J.; Fan, J. A. Global Optimization of Dielectric Metasurfaces Using a Physics-Driven Neural Network. *Nano Lett.* **2019**, *19* (8), 5366–5372. https://doi.org/10.1021/acs.nanolett.9b01857.
(63) Liu, W.; Liu, W.; Shi, L.; Kivshar, Y. Topological Polarization Singularities in Metaphotonics. *Nanophotonics* **2021**. https://doi.org/10.1515/nanoph-2020-0654.
(64) Engheta, N. Metamaterials with High Degrees of Freedom: Space, Time, and More. *Nanophotonics* **2021**, *10* (1), 639–642. https://doi.org/10.1515/nanoph-2020-0414.
(65) Meng, C.; Thrane, P. C. V.; Ding, F.; Gjessing, J.; Thomaschewski, M.; Wu, C.; Dirdal, C.; Bozhevolnyi, S. I. Dynamic MEMS-Based Optical Metasurfaces. *arXiv:2101.08834 [physics]* **2021**.
(66) Hong, X.; Hu, G.; Zhao, W.; Wang, K.; Sun, S.; Zhu, R.; Wu, J.; Liu, W.; Loh, K. P.; Wee, A. T. S.; Wang, B.; Alù, A.; Qiu, C.-W.; Lu, P. Structuring Nonlinear Wavefront Emitted from Monolayer Transition-Metal Dichalcogenides. *Research* **2020**, *2020*, 1–10. https://doi.org/10.34133/2020/9085782.
(67) Hu, G.; Shen, J.; Qiu, C.-W.; Alù, A.; Dai, S. Phonon Polaritons and Hyperbolic Response in van Der Waals Materials. *Advanced Optical Materials* **2020**, *8* (5), 1901393. https://doi.org/10.1002/adom.201901393.
(68) Hu, G.; Krasnok, A.; Mazor, Y.; Qiu, C.-W.; Alù, A. Moiré Hyperbolic Metasurfaces. *Nano Lett.* **2020**, *20* (5), 3217–3224. https://doi.org/10.1021/acs.nanolett.9b05319.
(69) Ma, W.; Alonso-González, P.; Li, S.; Nikitin, A. Y.; Yuan, J.; Martín-Sánchez, J.; Taboada-Gutiérrez, J.; Amenabar, I.; Li, P.; Vélez, S.; Tollan, C.; Dai, Z.; Zhang, Y.; Sriram, S.; Kalantar-Zadeh, K.; Lee, S.-T.; Hillenbrand, R.; Bao, Q. In-Plane Anisotropic and Ultra-Low-Loss Polaritons in a Natural van Der Waals Crystal. *Nature* **2018**, *562* (7728), 557–562. https://doi.org/10.1038/s41586-018-0618-9.
(70) Zheng, Z.; Chen, J.; Wang, Y.; Wang, X.; Chen, X.; Liu, P.; Xu, J.; Xie, W.; Chen, H.; Deng, S.; Xu, N. Highly Confined and Tunable Hyperbolic Phonon Polaritons in Van Der Waals Semiconducting Transition Metal Oxides. *Advanced Materials* **2018**, *30* (13), 1705318. https://doi.org/10.1002/adma.201705318.
(71) Dai, Z.; Hu, G.; Si, G.; Ou, Q.; Zhang, Q.; Balendhran, S.; Rahman, F.; Zhang, B. Y.; Ou, J. Z.; Li, G.; Alù, A.; Qiu, C.-W.; Bao, Q. Edge-Oriented and Steerable Hyperbolic Polaritons in Anisotropic van Der Waals Nanocavities. *Nature Communications* **2020**, *11* (1), 6086. https://doi.org/10.1038/s41467-020-19913-4.
(72) Lee, B.; Park, J.; Han, G. H.; Ee, H.-S.; Naylor, C. H.; Liu, W.; Johnson, A. T. C.; Agarwal, R. Fano Resonance and Spectrally Modified Photoluminescence Enhancement in Monolayer MoS2 Integrated with Plasmonic Nanoantenna Array. *Nano Lett.* **2015**, *15* (5), 3646–3653. https://doi.org/10.1021/acs.nanolett.5b01563.
(73) Dibos, A. M.; Zhou, Y.; Jauregui, L. A.; Scuri, G.; Wild, D. S.; High, A. A.; Taniguchi, T.; Watanabe, K.; Lukin, M. D.; Kim, P.; Park, H. Electrically Tunable Exciton–Plasmon Coupling in a WSe2 Monolayer Embedded in a Plasmonic Crystal Cavity. *Nano Lett.* **2019**, *19* (6), 3543–3547. https://doi.org/10.1021/acs.nanolett.9b00484.
(74) Huang, C.; Zhang, C.; Xiao, S.; Wang, Y.; Fan, Y.; Liu, Y.; Zhang, N.; Qu, G.; Ji, H.; Han, J.; Ge, L.; Kivshar, Y.; Song, Q. Ultrafast Control of Vortex Microlasers. *Science* **2020**, *367* (6481), 1018–1021. https://doi.org/10.1126/science.aba4597.
(75) Li, Z.; Smalley, J. S. T.; Haroldson, R.; Lin, D.; Hawkins, R.; Gharajeh, A.; Moon, J.; Hou, J.; Zhang, C.; Hu, W.; Zakhidov, A.; Gu, Q. Active Perovskite Hyperbolic Metasurface. *ACS Photonics* **2020**, *7* (7), 1754–1761. https://doi.org/10.1021/acsphotonics.0c00391.

(76) Folland, T. G.; Fali, A.; White, S. T.; Matson, J. R.; Liu, S.; Aghamiri, N. A.; Edgar, J. H.; Haglund, R. F.; Abate, Y.; Caldwell, J. D. Reconfigurable Infrared Hyperbolic Metasurfaces Using Phase Change Materials. *Nature Communications* **2018**, *9* (1), 4371. https://doi.org/10.1038/s41467-018-06858-y.
(77) Polk, C.; Postow, E. *Handbook of Biological Effects of Electromagnetic Fields, Third Edition - 2 Volume Set*; Boca Raton, FL, USA: CRC Press, 1996.
(78) Zeng, S.; Sreekanth, K. V.; Shang, J.; Yu, T.; Chen, C.-K.; Yin, F.; Baillargeat, D.; Coquet, P.; Ho, H.-P.; Kabashin, A. V.; Yong, K.-T. Graphene-Gold Metasurface Architectures for Ultrasensitive Plasmonic Biosensing. *Adv. Mater.* **2015**, *27* (40), 6163–6169. https://doi.org/10.1002/adma.201501754.
(79) Kabashin, A. V.; Evans, P.; Pastkovsky, S.; Hendren, W.; Wurtz, G.; Atkinson, R.; Pollard, R.; Podolskiy, V.; Zayats, A. Plasmonc Nanorod Metamaterials for Biosensing. *Nature materials* **2009**, *8*, 867–871. https://doi.org/10.1038/nmat2546.
(80) Sreekanth, K. V.; Alapan, Y.; ElKabbash, M.; Ilker, E.; Hinczewski, M.; Gurkan, U. A.; De Luca, A.; Strangi, G. Extreme Sensitivity Biosensing Platform Based on Hyperbolic Metamaterials. *Nature Materials* **2016**, *15* (6), 621–627. https://doi.org/10.1038/nmat4609.
(81) Goodman, J. W. *Introduction to Fourier Optics*; McGraw Hill, New York, 1968.
(82) Lin, R. J.; Su, V.-C.; Wang, S.; Chen, M. K.; Chung, T. L.; Chen, Y. H.; Kuo, H. Y.; Chen, J.-W.; Chen, J.; Huang, Y.-T.; Wang, J.-H.; Chu, C. H.; Wu, P. C.; Li, T.; Wang, Z.; Zhu, S.; Tsai, D. P. Achromatic Metalens Array for Full-Colour Light-Field Imaging. *Nature Nanotechnology* **2019**, *14* (3), 227–231. https://doi.org/10.1038/s41565-018-0347-0.
(83) Guo, Q.; Shi, Z.; Huang, Y.-W.; Alexander, E.; Qiu, C.-W.; Capasso, F.; Zickler, T. Compact Single-Shot Metalens Depth Sensors Inspired by Eyes of Jumping Spiders. *Proc Natl Acad Sci USA* **2019**, *116* (46), 22959–22965. https://doi.org/10.1073/pnas.1912154116.
(84) Makhsiyan, M.; Bouchon, P.; Jaeck, J.; Pelouard, J.-L.; Haïdar, R. Shaping the Spatial and Spectral Emissivity at the Diffraction Limit. *Appl. Phys. Lett.* **2015**, *107* (25), 251103. https://doi.org/10.1063/1.4937453.
(85) Song, M.; Wang, D.; Kudyshev, Z. A.; Xuan, Y.; Wang, Z.; Boltasseva, A.; Shalaev, V. M.; Kildishev, A. V. Enabling Optical Steganography, Data Storage, and Encryption with Plasmonic Colors. *Laser & Photonics Reviews* **2021**, *15* (3), 2000343. https://doi.org/10.1002/lpor.202000343.
(86) Liu, H.-C.; Yang, B.; Guo, Q.; Shi, J.; Guan, C.; Zheng, G.; Mühlenbernd, H.; Li, G.; Zentgraf, T.; Zhang, S. Single-Pixel Computational Ghost Imaging with Helicity-Dependent Metasurface Hologram. *Science Advances* **2017**, *3* (9), e1701477. https://doi.org/10.1126/sciadv.1701477.
(87) Zheng, P.; Dai, Q.; Li, Z.; Ye, Z.; Xiong, J.; Liu, H.-C.; Zheng, G.; Zhang, S. Metasurface-Based Key for Computational Imaging Encryption. *Science Advances* **2021**, *7* (21), eabg0363. https://doi.org/10.1126/sciadv.abg0363.
(88) Finlayson, E. D.; Hooper, I. R.; Lawrence, C. R.; Heath, M.; Anderson, D.; Sambles, J. R.; Vukusic, P. Covert Images Using Surface Plasmon-Mediated Optical Polarization Conversion. *Advanced Optical Materials* **2018**, *6* (5), 1700843. https://doi.org/10.1002/adom.201700843.
(89) Zhang, L.; Chen, X. Q.; Liu, S.; Zhang, Q.; Zhao, J.; Dai, J. Y.; Bai, G. D.; Wan, X.; Cheng, Q.; Castaldi, G.; Galdi, V.; Cui, T. J. Space-Time-Coding Digital Metasurfaces. *Nature Communications* **2018**, *9* (1), 4334. https://doi.org/10.1038/s41467-018-06802-0.
(90) Zhao, J.; Yang, X.; Dai, J. Y.; Cheng, Q.; Li, X.; Qi, N. H.; Ke, J. C.; Bai, G. D.; Liu, S.; Jin, S.; Alù, A.; Cui, T. J. Programmable Time-Domain Digital-Coding Metasurface for Non-Linear Harmonic Manipulation and New Wireless Communication Systems. *National Science Review* **2019**, *6* (2), 231–238. https://doi.org/10.1093/nsr/nwy135.

(91) Devlin, R. C.; Ambrosio, A.; Rubin, N. A.; Mueller, J. P. B.; Capasso, F. Arbitrary Spin-to–Orbital Angular Momentum Conversion of Light. *Science* **2017**, *358* (6365), 896–901. https://doi.org/10.1126/science.aao5392.
(92) Wang, D.; Liu, F.; Liu, T.; Sun, S.; He, Q.; Zhou, L. Efficient Generation of Complex Vectorial Optical Fields with Metasurfaces. *Light: Science & Applications* **2021**, *10* (1), 67. https://doi.org/10.1038/s41377-021-00504-x.
(93) Santiago-Cruz, T.; Fedotova, A.; Sultanov, V.; Weissflog, M. A.; Arslan, D.; Younesi, M.; Pertsch, T.; Staude, I.; Setzpfandt, F.; Chekhova, M. Photon Pairs from Resonant Metasurfaces. *Nano Lett.* **2021**, *21* (10), 4423–4429. https://doi.org/10.1021/acs.nanolett.1c01125.
(94) Kort-Kamp, W. J. M.; Azad, A. K.; Dalvit, D. A. R. Space-Time Quantum Metasurfaces. **2021**, *arXiv:2101.10433. [physics:quant-ph].* (25 Jan 2021).
(95) Solntsev, A. S.; Agarwal, G. S.; Kivshar, Y. Metasurfaces for Quantum Photonics. *Nature Photonics* **2021**, *15* (5), 327–336. https://doi.org/10.1038/s41566-021-00793-z.
(96) Sounas, D. L.; Alù, A. Non-Reciprocal Photonics Based on Time Modulation. *Nature Photonics* **2017**, *11* (12), 774–783. https://doi.org/10.1038/s41566-017-0051-x.
(97) Koshelev, K.; Lepeshov, S.; Liu, M.; Bogdanov, A.; Kivshar, Y. Asymmetric Metasurfaces with High-Q Resonances Governed by Bound States in the Continuum. *Phys. Rev. Lett.* **2018**, *121* (19), 193903. https://doi.org/10.1103/PhysRevLett.121.193903.
(98) Koshelev, K.; Bogdanov, A.; Kivshar, Y. Meta-Optics and Bound States in the Continuum. *Science Bulletin* **2019**, *64* (12), 836–842. https://doi.org/10.1016/j.scib.2018.12.003.
(99) Gorkunov, M. V.; Antonov, A. A.; Kivshar, Y. S. Metasurfaces with Maximum Chirality Empowered by Bound States in the Continuum. *Phys. Rev. Lett.* **2020**, *125* (9), 093903. https://doi.org/10.1103/PhysRevLett.125.093903.
(100) Zhu, L.; Liu, X.; Sain, B.; Wang, M.; Schlickriede, C.; Tang, Y.; Deng, J.; Li, K.; Yang, J.; Holynski, M.; Zhang, S.; Zentgraf, T.; Bongs, K.; Lien, Y.-H.; Li, G. A Dielectric Metasurface Optical Chip for the Generation of Cold Atoms. *Science Advances* **2020**, *6* (31), eabb6667. https://doi.org/10.1126/sciadv.abb6667.
(101) Abdollahramezani, S.; Hemmatyar, O.; Taghinejad, M.; Taghinejad, H.; Kiarashinejad, Y.; Zandehshahvar, M.; Fan, T.; Deshmukh, S.; Eftekhar, A. A.; Cai, W.; Pop, E.; El-Sayed, M. A.; Adibi, A. Dynamic Hybrid Metasurfaces. *Nano Lett.* **2021**, *21* (3), 1238–1245. https://doi.org/10.1021/acs.nanolett.0c03625.
(102) Wetzstein, G.; Ozcan, A.; Gigan, S.; Fan, S.; Englund, D.; Soljačić, M.; Denz, C.; Miller, D. A. B.; Psaltis, D. Inference in Artificial Intelligence with Deep Optics and Photonics. *Nature* **2020**, *588* (7836), 39–47. https://doi.org/10.1038/s41586-020-2973-6.

Graphical TOC image